



# Classification of seismic events using linear discriminant function (LDF) in the Sakarya region, Turkey

Emrah Budakoğlu<sup>1</sup> · Gündüz Horasan<sup>1</sup>

Received: 4 January 2018 / Accepted: 12 July 2018 / Published online: 18 July 2018  
© Institute of Geophysics, Polish Academy of Sciences & Polish Academy of Sciences 2018

## Abstract

The Sakarya prefecture is an interesting area with various seismicity types. This activity comes from earthquakes occurring at the North Anatolian Fault Zone and from a few quarry blast areas in the region. These quarry blast recordings produce errors in the determination of active faults and mapping of the microearthquake activity. Therefore, to recognize the tectonic activity in the region, we need to be able to discriminate between earthquakes and quarry blasts in the catalogues. In this study, a statistical analysis method (linear discriminant function) has been applied to classify seismic events occurring in the Sakarya region. We used 110 seismic events that were recorded by Sakarya University Seismic Station between 2012 and 2014. Time and frequency variant parameters, maximum S wave and maximum P wave amplitude ratio ( $S/P$ ), the spectral ratio ( $S_r$ ), maximum frequency ( $f_{max}$ ), and total signal duration of the waveform were used for discrimination analyses. The maximum frequency ( $f_{max}$ ) versus time duration of the seismic signal gives a higher classification percentage (94%) than the other discriminants. At the end of this study, 41 out of 110 events (44%) are determined as quarry blasts, and 62 (56%) are considered as earthquakes.

**Keywords** Classification · Earthquake · Quarry blast · LDF · Sakarya

## Introduction

The North Anatolian Fault Zone (NAFZ) is located at the south of the Adapazarı basin (Fig. 1) and is the main source of the seismicity of the Sakarya region. A few quarry blast areas were determined by field observations and satellite images from the Google Earth program. Today, the quarries operating at the Geyve and Akyazı, Taraklı and Pamukova, and Ferizli and Söğütü districts (boxed areas in Fig. 1) regularly contaminate the seismograms recorded by Bogazici University Kandilli Observatory and Earthquake Research Institute, Regional Earthquake–Tsunami Monitoring Center (KOERI-RETMC). We should not use earthquake data together with explosions for risk analyses. Therefore, the earthquake catalogues should be cleaned by removing these quarry blast records. In recent years, quarry blast events are discriminated automatically by KOERI.

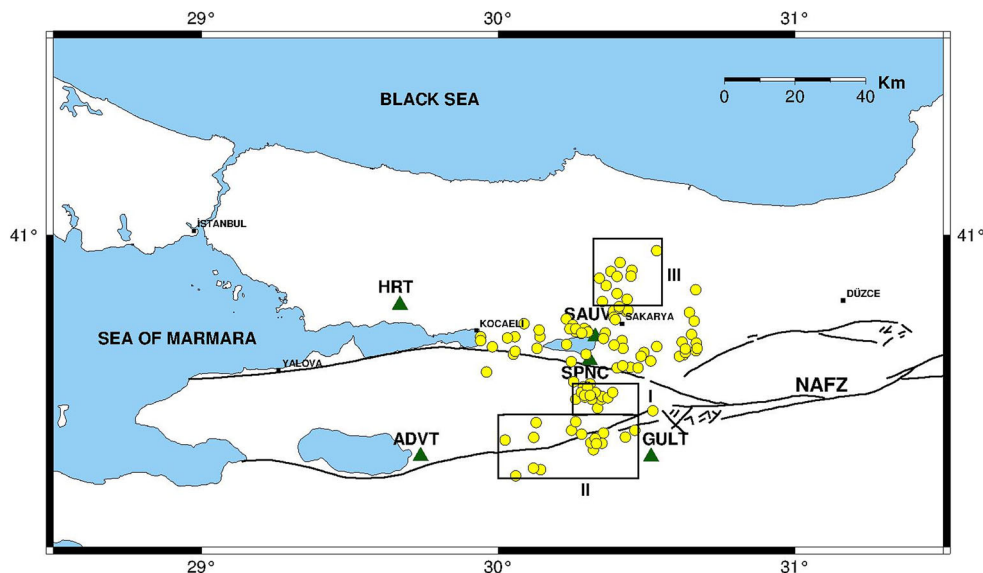
However, these events were not automatically discriminated by KOERI between 2012 and 2014 at the Sakarya prefecture.

Various methods are used by researchers to classify earthquakes and quarry blasts. Wiemer and Baer (2000), Gulia (2010), and Kekovalı et al. (2011) used daytime hours to discriminate explosions from earthquakes. A large number of studies have identified short period discriminations for particular regions. The most popular discriminator is the  $S/P$  ratio (Baumgardt and Young 1990; Taylor et al. 1989; Wüster 1993; Horasan et al. 2009; Yılmaz et al. 2013). The spectral representation of some wave groups or spectral ratios of seismic phases or spectrograms have been used as discriminants for different seismic events (Hedlin et al. 1989; Hedlin et al. 1990; Chernobay and Gabsatarova 1999; Koch and Fah 2002; Allmann et al. 2008; Dahy and Hassib 2010; Hammer et al. 2013). Ataeva et al. (2017) used the  $f_0(P)/f_0(S)$  corner frequencies ratio of the spectrum as a discriminant for seismic events in Israel and Lebanon. Their study indicated that the corner frequencies of quarry blast events were lower than those of earthquakes.

✉ Gündüz Horasan  
ghorasan@sakarya.edu.tr

<sup>1</sup> Department of Geophysical Engineering, Faculty of Engineering, Sakarya University, Sakarya 54187, Turkey

**Fig. 1** Map shows seismic events (filled yellow-colored circles) and seismic stations (filled green-colored triangles) between 2012 and 2014 in the study area. Boxes show the sites of quarries producing the main quarry blast activity (I, Geyve and Akyazı district; II, Taraklı and Pamukova district; III, Ferizli and Söğütli district) determined from satellite images and field observations. NAFZ: North Anatolian Fault Zone



In Switzerland, Hammer et al. (2013) automatically classified seismic events according to a statistical classifier called hidden Markov models. Another automatic classification of seismic events was made by Kortstöröm et al. (2016) in Finland. These authors used a supervised pattern recognition technique (SVM) for classification and obtained a 6% false alarm rate. Kiszely and Györi (2015) made a waveform similarity analysis (based on correlation analysis) to separate earthquakes and explosions at the Vertes Hill in Hungary.

The earthquake and quarry blast events are produced by different energy sources. Faults are formed by cracking of the Earth's crust by pairs of opposite forces, whereas the quarry blasts are formed by equivalent forces applied in all directions. The waveforms at different stations of an earthquake that occurred on November 10, 2013, are shown in Fig. 2. The first motion polarity of an earthquake can be upward or downward because of the seismic stations located at different azimuth degrees. Figure 3 shows the seismic waveforms of the quarry blast at three stations. It can be seen that the first motion polarity is always upward at all stations, thus confirming the explosive nature of the recorded event.

In this study, to distinguish between tectonic earthquakes and quarry blasts, we discriminated the events at Sakarya prefecture, Turkey, in terms of time and frequency domain analyses of digital seismograms. One of the main problems occurring in seismic source classification is the misclassification of the events. To prevent misclassification of the events, we used direct P and S waves only at one station instead of the whole network. The longer the distance of the station from epicenter, the more complex will be the seismogram. So we reduced wave path and distance effects using only one near station.

## Tectonics

The NAFZ is a well-known strike-slip fault on Earth. The North Anatolian Fault separates into three fault strands in the Marmara region (Fig. 4) (Barka and Kadinsky-Cade 1988; Emre et al. 2013). The Northern strand goes under the Sapanca-Cinarcik-Marmara Sea and enters the Saros Gulf. The Middle strand follows the Osmanieli-Gemlik-Bandırma-Bayramic line and continues on its way. The Southern strand goes through the Geyve-Yenişehir-Bursa-Biga Peninsula line and enters the North Aegean Sea. Thus, the active tectonics of the Marmara region is controlled by the NAFZ. Global Positioning System studies (Reilinger et al. 2006; Pondard et al. 2007) suggest that the greatest slip rate between the three strands is at the north branch, slipping 20 mm/year. For the Middle and South strands, the calculated fault slip rates are 3 and 2 mm/year, respectively. When these three strands reach a plate movement of about 25 mm/year, there is a significant earthquake hazard risk of the Marmara region. The most important evidence of this earthquake hazard risk is the large and continuous small earthquakes that took place during the historical and instrumental seismicity period (Ambraseys 2001, 2009; Nalbant et al. 1998; Caputo et al. 2012). Two strong earthquakes occurred in the Marmara region on 1999: the August 17, Mw 7.5 Izmit earthquake, and the November 12, Mw 7.2 Düzce earthquake. The Izmit earthquake of August 17, 1999, occurred on the northern strand of the North Anatolian Fault, and focal mechanism solutions indicate pure right-lateral strike-slip faulting (Gülen et al. 2002; Harvard CMT 2018). The November 12, 1999, the Düzce earthquake occurred nearly 3 months after the İzmit earthquake, and the focal

**Fig. 2** Seismograms of November 10, 2013, 02:09:23.4 GMT earthquake. The first motion polarity is upward for GULT, HRT, and ADVT station records, whereas it is downward for the SAUV and SPNC station records

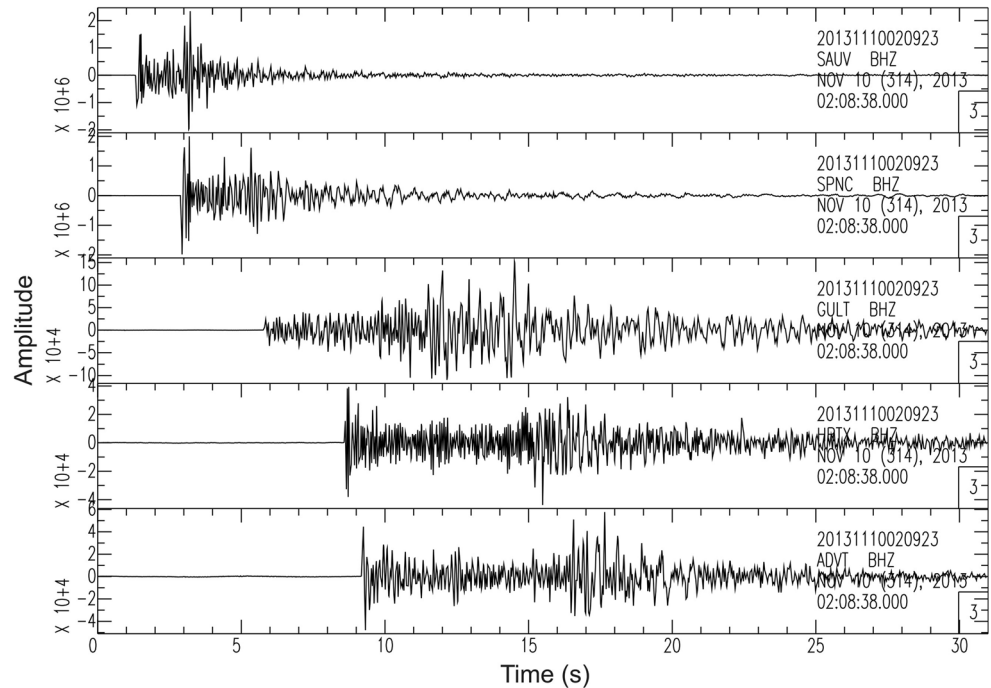
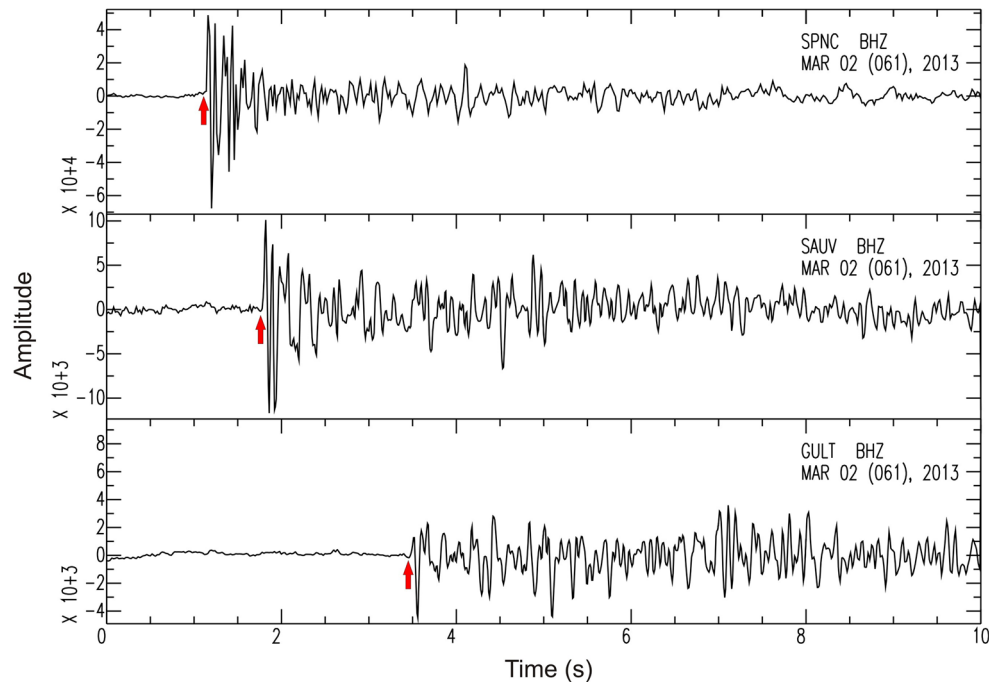


**Fig. 3** Seismograms of March 2, 2013, 13:23:46 GMT quarry blast recorded at three stations. The first motion polarity is upward at all station records



mechanism solutions show predominantly right-lateral strike-slip faulting with a small normal faulting component (Tibi et al. 2001; Harvard CMT 2018). These two destructive earthquakes caused huge economic losses and casualties. For this reason, earthquake hazard studies are important in the Marmara region.

## Method and data analysis

One hundred ten seismic events that occurred in Sakarya region were analyzed. Events were selected within 50 km from Sakarya University (SAUV) seismic station. The epicenter locations of the events were calculated by KOERI-RETMC. The seismic event distributions are shown in Fig. 1. We used events with magnitude ( $M_L$ )

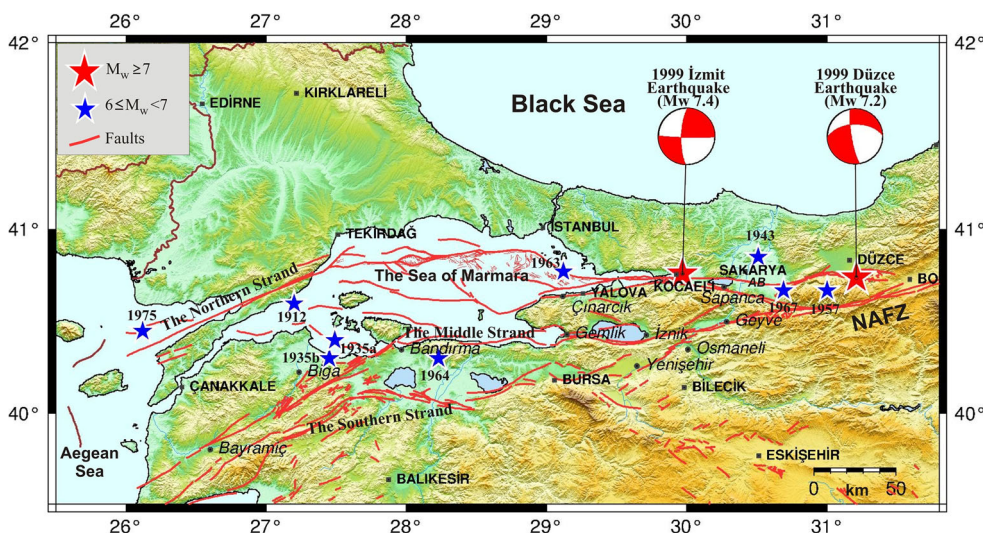


**Fig. 4** The simple regional active tectonic map of Marmara region and its surroundings. Earthquakes have occurred in the instrumental period, indicated by stars [epicenters of earthquakes were obtained at Kandilli Observatory and Earthquake Research Institute Regional Earthquake–Tsunami Monitoring Center (KOERI-RETMC)]. Source

mechanisms (red-white beach balls) of August 17, 1999, İzmit and November 12, 1999, Düzce earthquakes were obtained from Harvard CMT catalog. Faults were taken from Şaroğlu et al. (1992), Emre et al. (2013), and Yaltırak et al. (2012). NAFZ: North Anatolian Fault Zone, AB: Adapazarı Basin

between 1.5 and 2.8 that occurred during 2012 and 2014. Only four seismic events with  $3.0 \leq M_L \leq 4.0$  have been recorded in the period from 2012 to 2013: the first ( $M_L = 4.0$ ) on the July 7, 2012, at Köprübaşı-Adapazarı; the second ( $M_L = 3.8$ ) on December 9, 2012, at Yayalar-Hendek; the third ( $M_L = 3.4$ ) on April 23, 2013, at Serdivan-Adapazarı; and the fourth ( $M_L = 3.2$ ) on June 30, 2013, at Akyazı-Sakarya. In this study, the SAUV seismic station’s data were used for time and frequency domain analysis. The SAUV seismic station was installed in 2012 and is operated by Sakarya University and KOERI-RETMC. The station of SAUV is a three-component broadband seismic station whose sampling rate is 100 samples per second.

In this study, temporal distribution, waveform analyses, and spectral analyses are performed for earthquake and quarry blast data. In the temporal distribution of seismicity as a function of hours of the day (Fig. 5), we observed a high seismic activity between 12 a.m. and 4 p.m. GMT. This histogram shows that the quarry blasts occur periodically in the daytime. Daytime and nighttime hours are insufficient to classify earthquakes and quarry blasts in these regions. Therefore, we used waveform and spectrum information of the events for discrimination. Maximum amplitude peak ratio, spectral amplitude ratio, maximum frequency, and time duration of the seismic signal were selected as discriminants for this study.

In the waveform analysis, we determined maximum P wave and maximum S wave amplitude values from the velocity seismograms of earthquakes and quarry blasts. The vertical component of velocity seismogram of the earthquake and the quarry blast is shown in Fig. 6a, b.

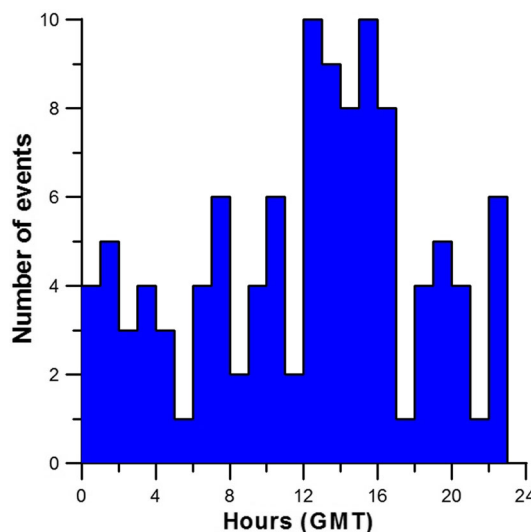


**Fig. 5** Time–frequency distribution of seismic events between 2012 and 2014 (filled circles in Fig. 1). Times in GMT

Then, we calculated the S/P maximum amplitude peak ratio and plotted these values against the logarithm of amplitude peak of S wave ( $\log S$ ).

In the spectral analysis, we used multiple parameters, including the spectral amplitude ratio and maximum frequency of the spectrum. The frequency contents of the events that were used in this study are shown in Figs. 7a, b, 8, and 9. The amplitude spectra were calculated using the fast Fourier transform (FFT) method. In the spectral analysis, the spectral ratio ( $S_r$ ) versus the maximum frequency ( $f_{max}$ ) of the spectrum was plotted.  $S_r$  is the ratio of



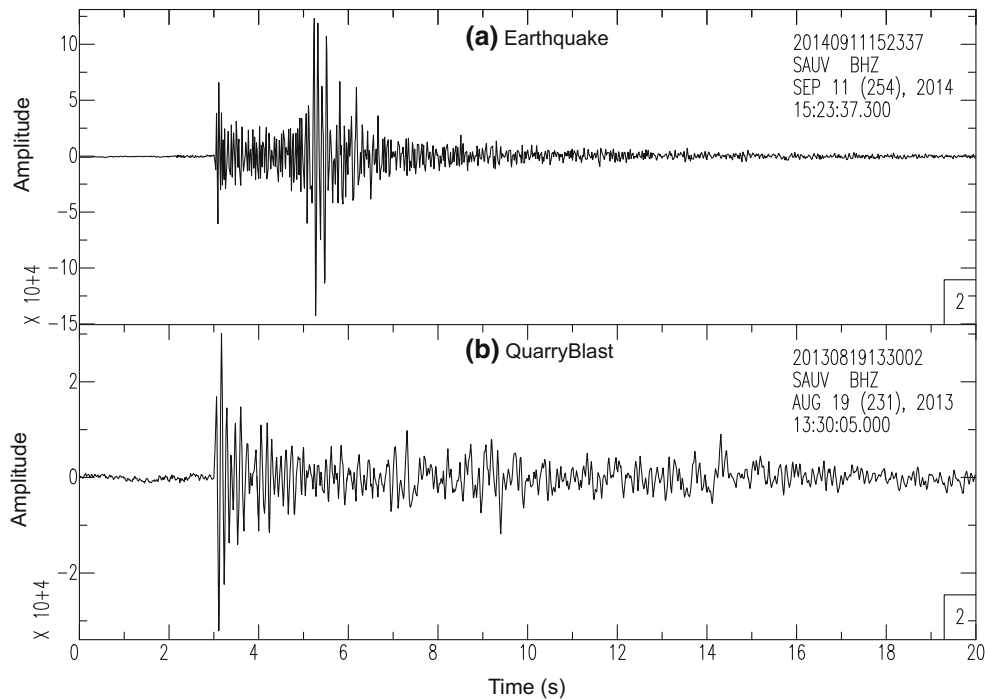


**Fig. 6** The vertical components of the velocity seismograms with a time window length of 20 s for **a** an earthquake and, **b** a quarry blast recorded at SAUV

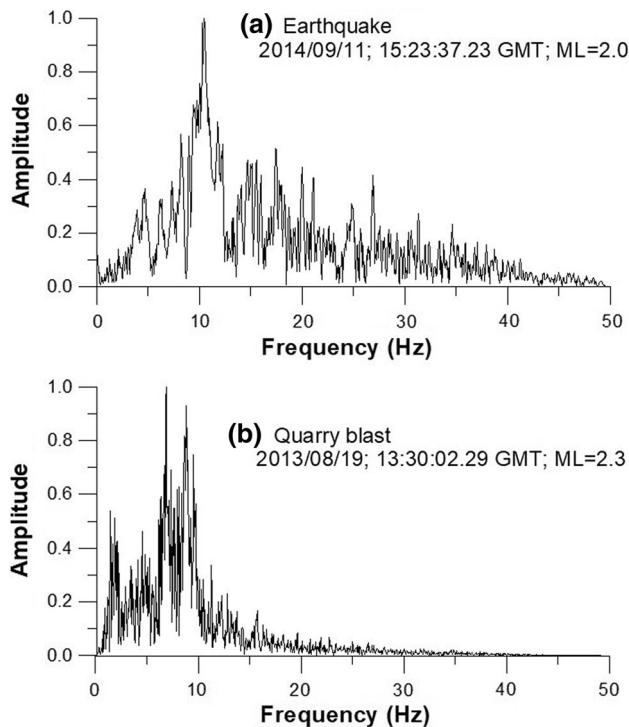


**Fig. 7** Normalized amplitude spectra for **a** earthquake and **b** quarry blasts recorded at SAUV

spectrum amplitudes  $a(f)$ , which is the spectral amplitude of the velocity of the ground motion (Gitterman and

Shapira 1993). Spectral amplitude ratio ( $Sr$ ) is calculated in Eq. (1).

$$Sr = \frac{\int_{h_1}^{h_2} a(f) df}{\int_{l_1}^{l_2} a(f) df} \quad (1)$$

We determined high-frequency limit values ( $h_1$ – $h_2$ ) as 10–20 Hz and low-frequency limit values ( $l_1$ – $l_2$ ) as 1–10 Hz from the spectrum. Our observations and other studies (Allmann et al. 2008; Hammer et al. 2013) show that the earthquakes have a wider frequency bandwidth than quarry blasts. Therefore, we decided to use maximum frequency values of the spectrum as a variant parameter.

We also obtained spectrograms for each event using the Seismic Analysis Code (SAC 2000) to gain more information about the frequency (Figs. 8, 9). A spectrogram is a visual way of representing the signal strength of a signal over time at various frequencies present in a particular waveform. The seismic signals in Figs. 8 and 9 show strong energies associated with the arrivals of P and S waves.

Next, we used both time and spectrum parameters for the discrimination analysis. We plotted the maximum frequency versus time duration of the seismic events on the seismogram.

The seismic events were statistically analyzed using amplitude peak ratio, spectral ratio, maximum frequency, and time duration of the seismic events. Linear

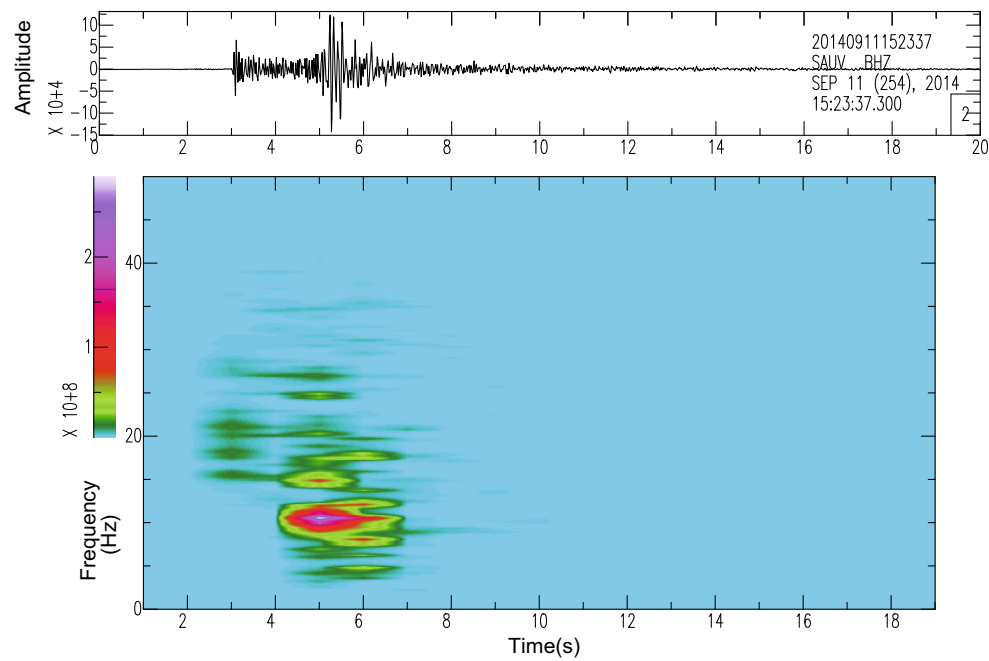


**Fig. 8** Example of the spectrogram for an earthquake. The spectrogram is computed from the vertical component of the waveform. Purple, red, and light green colors present high energy contents, whereas dark green and turquoise colors present low energy contents

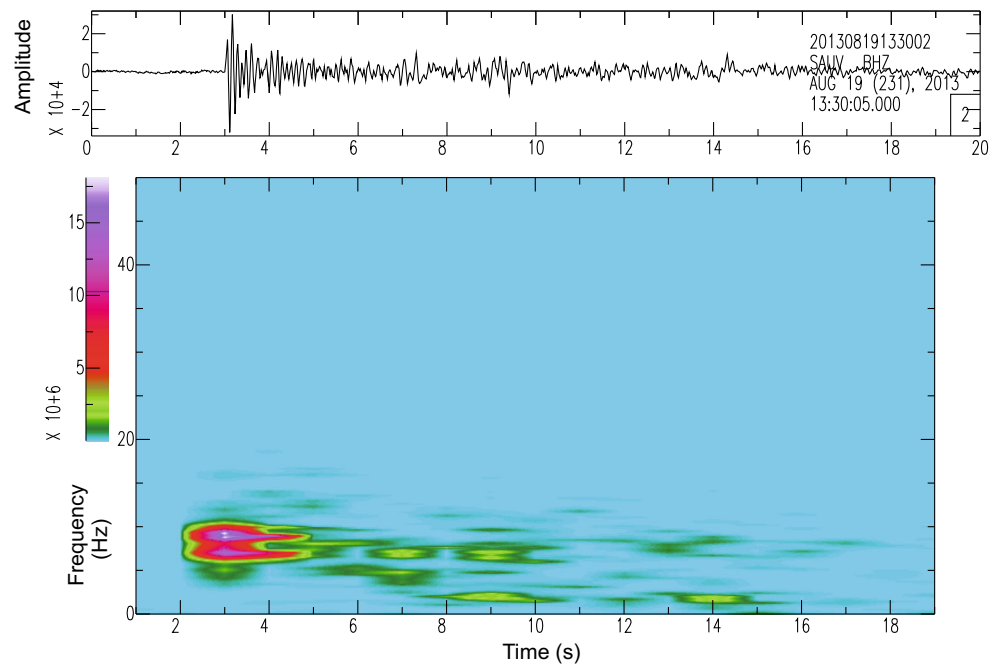


**Fig. 9** Example of the spectrogram for a quarry blast. The spectrogram is computed from the vertical component of the waveform. Purple, red, and light green colors present high energy contents, whereas dark green and turquoise colors present low energy contents

discriminant function (LDF) was used to discriminate different events (Fisher 1936).

In general, the LDFs can be demonstrated simply, as below:

$$F_{\text{LDF}} = a + b_1x_1 + b_2x_2 + \dots + b_mx_m \quad (2)$$

where  $a$  is a constant,  $b_1$  through  $b_m$  are regression coefficients, and  $x_1$  is the standardized value of the  $x_m$  discriminating variables. The interpretation of the results of a two-group problem is straightforward and closely follows the logic of multiple regressions.

In this study, statistical analysis was done with Statistical Package for the Social Sciences (SPSS v21 2012) software. This procedure estimates the coefficients, and the resulting function can be used to classify different events.

## Results

The presence of quarries in an active seismic zone might cause misinterpretation of the distribution of microseismicity. Statistically, three criteria were used for discrimination analysis between quarry blasts and earthquakes at Sakarya region, Turkey. The first criterion was obtained from the plot of the amplitude peak ratio of the S to P wave versus the logarithm of the S wave's amplitude peak in the time domain of the seismograms. The S/P amplitude ratios and logS values are plotted in Fig. 10. We have discriminated earthquakes from quarry blasts using the linear discrimination function (LDF) analysis. The discrimination line was obtained using SPSS software. The S/P amplitude ratios were generally larger for earthquakes than quarry blasts, but observations showed a little scattering in Fig. 10. We obtained a classification percentage of 91% for the events group using this statistical method.

The second criterion was obtained from the plot of the spectral ratio ( $Sr$ ) versus the maximum frequency ( $f_{\max}$ ) of

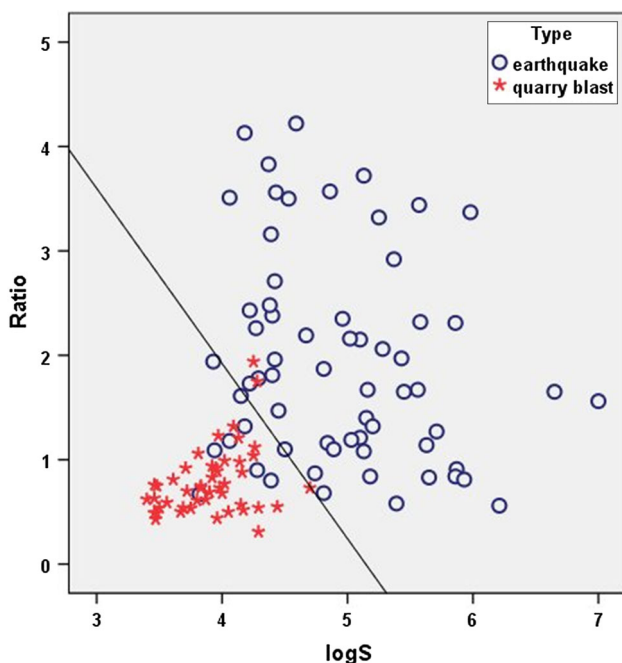


**Fig. 10** Plot of the amplitude peak ratio of S to P wave versus the logarithm of the S wave's amplitude peak ( $\log S$ ) of the vertical component seismograms for the investigated seismic events that were located in Sakarya. The discrimination line that separates the earthquakes from the quarry blasts has been determined from the linear discrimination function (LDF)

the spectrum. In Fig. 11 the spectral ratio is plotted against the maximum frequency for the seismic events in Sakarya region. According to these variables, we obtained a 93% classification percentage.

As the third criterion, we used the spectral and waveform analysis parameters together. We plotted the maximum frequency ( $f_{\max}$ ) versus the time duration of the seismic signal on the seismogram in Fig. 12. By this approach, the classification percentage is 94%. Table 1 shows the result of discriminant analysis between earthquakes and quarry blasts based on parameters presented in Fig. 12.

In addition to the criteria mentioned above, the Rg waves can be used for discriminant analysis of quarry blasts. The Rg waves are often observed on the vertical component seismograms of explosions or of very shallow earthquakes. We identified Rg waves on the seismograms of quarry blasts, and this was used as an observable discriminant. A good example is shown in Fig. 13, collected by the SAPNC Seismic Station.

In this study, we analyzed the P and S wave displacement spectra for an earthquake and a quarry blast with similar magnitude (Fig. 14). The analysis shows lower corner frequencies ( $f_c$ ) of explosions than earthquakes for the P and S wave.

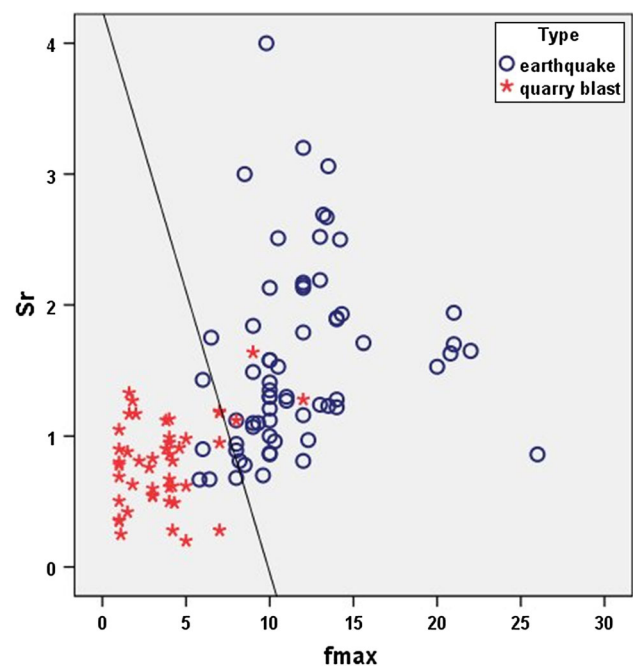


**Fig. 11** The plot of the maximum frequency ( $f_{\max}$ ) versus the spectral ratio ( $Sr$ ) of the vertical component seismograms for the investigated seismic events that were located in Sakarya. The discrimination line that separates the earthquakes from the quarry blasts has been determined from the linear discrimination function (LDF)

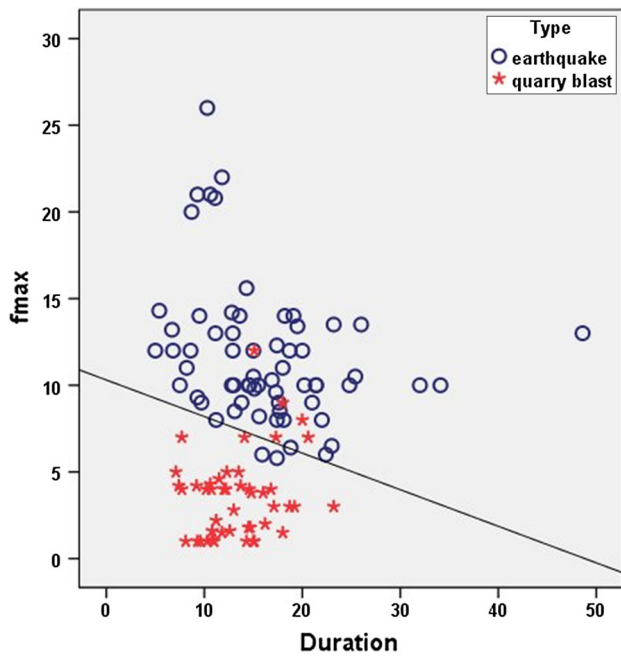


**Fig. 12** The plot of the maximum frequency ( $f_{max}$ ) of the spectrum versus the time duration of the vertical component seismograms for the investigated seismic events that were located in Sakarya. The discrimination line that separates the earthquakes from the quarry blasts has been determined from the linear discrimination function (LDF)

### Discussion and conclusions

The time and frequency features of earthquake and quarry blast signals are different. The vertical component of velocity seismogram of earthquakes and quarry blasts recorded at Sakarya region is shown in Fig. 6a, b. The P

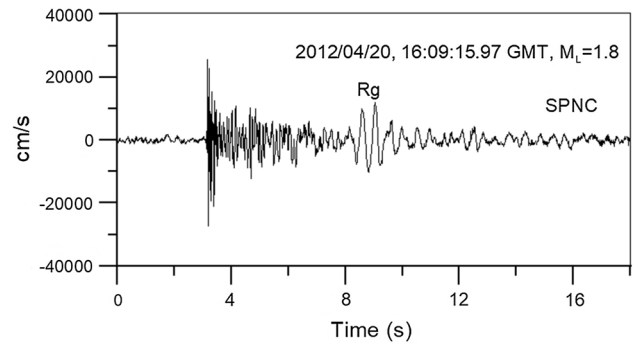


**Fig. 13** An example of Rg phase on a quarry blast seismogram recorded at the SPNC station. Seismic event located in the boxed area II in Fig. 1

wave amplitude relative to S wave amplitude in the vertical component seismogram is dominant for the quarry blasts, whereas earthquakes have a much larger S wave amplitude because quarry blast sources do not produce S waves.

The frequency contents of the events that were used in this study are shown in Figs. 7a, b, 8, and 9. In both the spectrum and spectrogram, earthquakes have a wider frequency content than quarry blasts. Hammer et al. (2013) and Allmann et al. (2008) have shown that the seismograms of quarry blasts are poorer in the high frequencies than corresponding earthquakes in their investigated data set. For economic and safety reasons, the quarry blasts often consist of several delayed blasts. This is called ripple firing or delayed shooting. The multiple explosions modulate the spectrum of the signal. Hedlin et al. (1989) and Kim et al. (1994) used this property to discriminate between ripple-fired quarry blasts and earthquakes. As seen in the spectrogram of the SAUV, record in Fig. 9 has

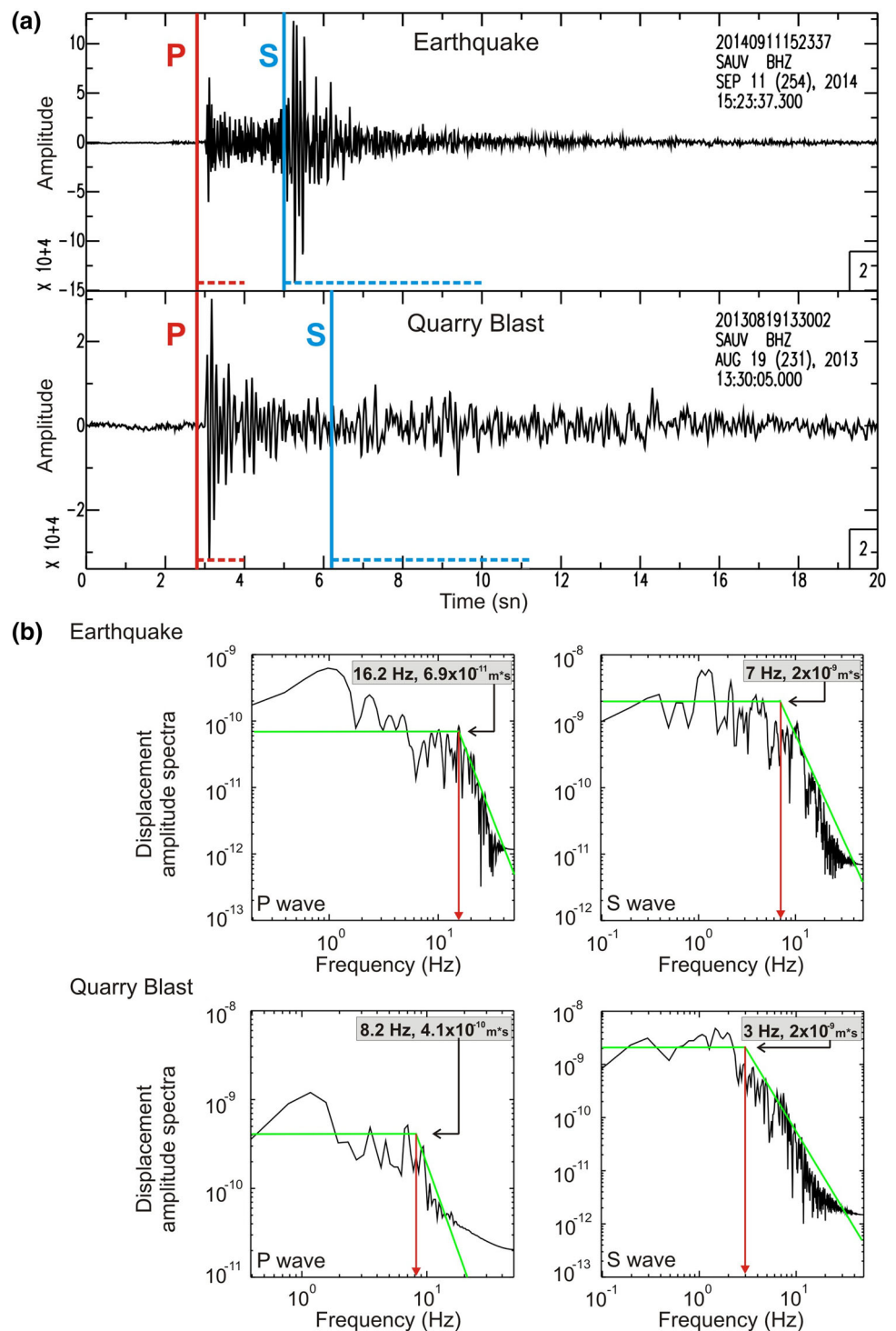
**Table 1** The results of the discriminant analysis methods between the earthquakes and the quarry blasts in Sakarya region (Fig. 1), which were based on the parameters presented in Figs. 10, 11, and 12

Criterion	Type	Predicted group membership		Total	
		Earthquake (E)	Quarry blast (QB)		
1	Original count	E	56	8	64
		QB	2	44	46
	%	E	87.5	12.5	100
		QB	4.3	95.7	100
2	Original count	E	59	5	64
		QB	3	43	46
	%	E	92.2	7.8	100
		QB	6.5	93.5	100
3	Original count	E	62	2	64
		QB	5	41	46
	%	E	96.9	3.1	100
		QB	10.9	89.1	100

Of the original grouped cases, 91, 93, and 94% were correctly classified at the Sakarya region for three criteria, respectively. Criteria: 1 ( $S/P$  amplitude ratio versus  $\log S$ ), 2 (spectral ratio ( $S_r$ ) versus the maximum frequency ( $f_{max}$ )), 3 (maximum frequency ( $f_{max}$ ) versus the time duration of the seismic signal)



**Fig. 14 a** An earthquake of 2014/09/11 ML 2.0, and a quarry blast of 2013/08/19, ML 2.3. The analyzed time windows of P and S wave trains are marked by red and blue broken lines, respectively.  
**b** Uncorrected P wave and S wave displacement spectra from seismograms of station SAUV. The green lines indicate the low-frequency amplitude level and high-frequency decay. The red line indicates the value of the corner frequency



modulation with a minimum around 7–8 Hz. Although we have two peaks in this case, it can be more than two. In this study, this property was also used for discrimination of quarry blasts from earthquakes. In Fig. 8, the spectrogram of the earthquake record shows a strong S wave amplitude at low frequencies (about 10 Hz), whereas the P wave

amplitude is between 15 and 28 Hz and significantly smaller than the S wave amplitude.

In this study, we used time and frequency domain parameters for discrimination analysis between quarry blasts and earthquakes at Sakarya region, Turkey. In the waveform analysis, the S/P maximum amplitude peak ratio and the log S were calculated for the events. The S/P values

are plotted versus the  $\log S$  values of the events in Fig. 10. The discrimination line is obtained using SPSS software. SPSS counts how many events within each group are correctly classified and how many are misclassified. The S/P amplitude ratios were generally larger for earthquakes than blasts, but observations show a little scattering. The distribution of the amplitude ratios shows overlap between 0.65 and 1.9 in Fig. 10. Some observations in the past showed an overlap in the earthquake and explosion data for some countries (Taylor et al. 1989). Another group of researchers obtained good results for the distribution of the amplitude ratios of the different phases (Bennett and Murphy 1986; Horasan et al. 2009; Ögütçü et al. 2011). The accuracy of the results depends on the geological features and source type in different regions (Zeiler and Velasco 2009). In this study, we obtained a classification percentage of 91% for the events group using the statistical method.

In the spectral analysis, the spectral ratio ( $S_r$ ) and the maximum frequency ( $f_{\max}$ ) values were used as the discriminant parameters. In Fig. 11, the spectral ratio is plotted versus the maximum frequency for the seismic events in Sakarya region. The two frequency bands for  $S_r$  were selected as high ( $h_1-h_2$ ; 10–20 Hz) and low ( $l_1-l_2$ ; 1–10 Hz) frequency bands. When we look at Fig. 11, we see that the frequency content of the earthquakes has a wider bandwidth than the quarry blasts. This property is also detected in Figs. 7a, b, 8 and 9. As seen in Fig. 11, the earthquakes and quarry blasts show little overlap. According to these variables, we obtained a 93% classification percentage using SPSS software.

As the third method, we used the spectral and waveform analysis parameters together. For these calculations, we plotted the maximum frequency ( $f_{\max}$ ) versus the time

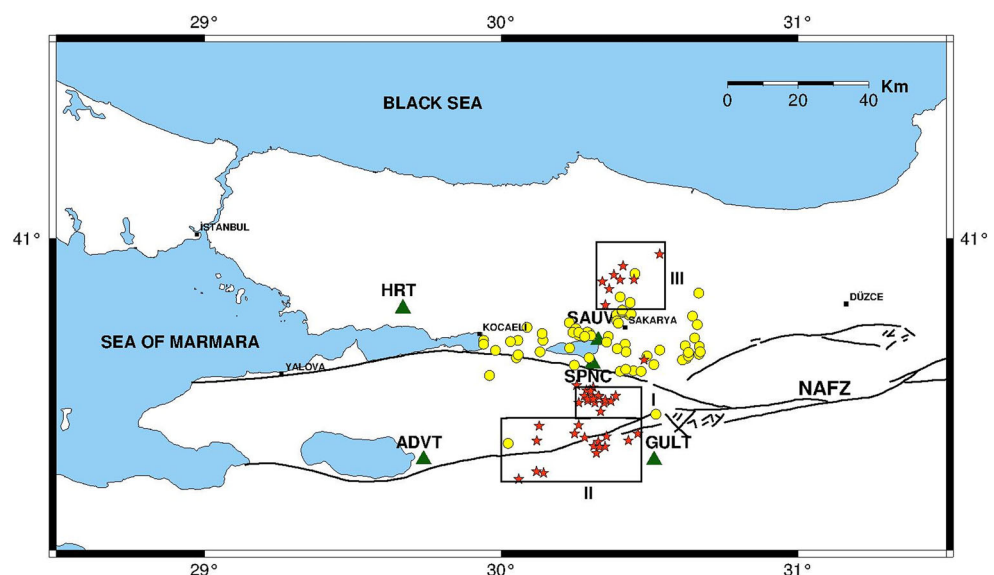
**Table 2** Comparison of the accuracy of criteria

Criterion	Number of total correctly classified events	Number of total misclassified events	Total accuracy (%)
1	100	10	91
2	102	8	93
3	103	7	94

duration of the seismic signal on the seismogram (Fig. 12). The earthquakes should have a longer duration than explosions because of the spatial and temporal dimension. According to the variables in Fig. 12, the classification percentage is 94% for seismic events. These statistical values are given in Table 1 for three criteria. In the first criterion in Table 1, 56 earthquakes out of 64 are classified correctly and 8 earthquakes are misclassified as quarry blasts, whereas 44 quarry blasts are classified correctly and 2 quarry blasts are misclassified as earthquakes. In the second criterion, 59 earthquakes out of 64 earthquakes are classified correctly and 5 earthquakes are misclassified as quarry blasts, whereas 43 quarry blasts are classified correctly and 3 quarry blasts are misclassified as earthquakes. In the third criterion in Table 1, 62 earthquakes out of 64 earthquakes are classified correctly and 2 earthquakes are misclassified as quarry blasts, whereas 41 quarry blasts are classified correctly and 5 quarry blasts are misclassified as earthquakes.

The number of total misclassified and correctly classified events and total accuracy of the analysis are shown in Table 2. For our case we can say that the third criterion (maximum frequency ( $f_{\max}$ ) versus the time duration of the seismic signal) is the best of all three.

**Fig. 15** Location map of earthquakes (filled yellow-colored circles), quarry blasts (filled red-colored stars), and broadband stations (filled green-colored triangles) of Boğaziçi University Kandilli Observatory and Earthquake Research Institute, Regional Earthquake–Tsunami Monitoring Center (KOERI-RETMC). Boxes show the sites of quarries producing main quarry blast activity (I, Geyve and Akyazı district; II, Taraklı and Pamukova district; III, Ferizli and Söğütü district) determined from satellite data and field observations. NAFZ, North Anatolian Fault Zone



As a result of our statistical analyses, the percentage of the blast and the earthquake classifications are 44 and 56%, respectively. The quarry blast and earthquake locations are shown in Fig. 15 (star: quarry blast, circle: earthquake) after discrimination analysis. This classification will help to determine the real seismicity of the region for future tectonic studies and seismic risk analysis.

**Acknowledgements** We thank Dr. Deniz Çaka for his valuable contribution. We thank anonymous reviewers for their constructive reviews and suggestions.

## References

- Allmann BP, Shearer PM, Hauksson E (2008) Spectral discrimination between quarry blasts and earthquakes in southern California. *Bull Seismol Soc Am* 98(4):2073–2079
- Ambraseys NN (2001) Reassessment of earthquakes, 1900–1999, in the Eastern Mediterranean and the Middle East. *Geophys J Int* 145:471–485
- Ambraseys NN (2009) Earthquakes in the eastern Mediterranean and the Middle East: a multidisciplinary study of 2,000 years of seismicity. Cambridge University Press, Cambridge
- Ataeva G, Gitterman A, Shapira A (2017) The ratio between corner frequencies of source spectra of P- and S-waves—a new discriminant between earthquakes and quarry blasts. *J Seismol* 21:209–220
- Barka A, Kadinsky-Cade K (1988) Strike-slip fault geometry in Turkey and its influence on earthquake activity. *Tectonics* 7:663–684
- Baumgardt DR, Young GB (1990) Regional seismic waveform discriminates and case-based event identification using regional arrays. *Bull Seismol Soc Am* 80:1874–1892
- Bennett TJ, Murphy JR (1986) Analysis of seismic discrimination capabilities using regional data from western United States events. *Bull Seismol Soc Am* 76:1069–1086
- Caputo R, Chatzipetors A, Pavlides S, Sboras S (2012) The Greek Database of Siesmogenic Sources (GreDaSS): state-of-the-art for northern Greece. *Ann Geophys* 55:5. <https://doi.org/10.4401/ag-5168>
- Chernobay IP, Gabsatarova IP (1999) Source classification in the Northern Caucasus. *Phys Earth Planet Inter* 113:183–201
- Dahy SA, Hassib GH (2010) Spectral discrimination between quarry blasts and microearthquakes in southern Egypt. *Res J Earth Sci* 2(1):1–7
- Emre Ö, Duman TY, Özalp S, Elmacı H, Olgun Ş, Şaroğlu Ş (2013) Active Fault Map of Turkey with Explanatory Text, General Directorate of Mineral Research and Exploration, Special Publication Series 30. Ankara, Turkey
- Fisher RA (1936) The use of multiple measurements in taxonomic problems. *Ann Eugen* 7:179–188
- Gitterman Y, Shapira A (1993) Spectral discrimination of underwater explosions. *Isr J Earth Sci* 42:37–44
- Gülen L, Pinar A, Kalafat D, Ozel N, Horasan G, Yilmazer M, İşikara AM (2002) Surface fault breaks, aftershock distribution, and rupture process of the 17 August 1999 Izmit, Turkey, earthquake. *Bull Seismol Soc Am* 92:230–244
- Gulia L (2010) Detection of quarry and mine blast contamination in European regional catalogues. *Nat Hazards* 53:229–249
- Hammer C, Ohrnberger M, Fah D (2013) Classifying seismic waveforms from scratch: a case study in the alpine environment. *Geophys J Int* 192:425–439. <https://doi.org/10.1093/gji/ggs036>
- Harvard Centroid Moment Tensor Catalog (Harvard CMT) 2018. <http://www.globalcmt.org/CMTsearch.html>. Accessed 3 May 2018
- Hedlin MA, Minster JB, Orcutt JA (1989) The time-frequency characteristics of quarry blasts and calibration explosions recorded in Kazakhstan. *USSR Geophys J* 99:109–121
- Hedlin M, Minster JB, Orcutt JA (1990) An automatic means to discriminate between earthquakes and quarry blasts. *Bull Seismol Soc Am* 80:2143–2160
- Horasan G, Boztepe-Güney A, Küsmezer A, Bekler F, Ögütçü Z, Musaoğlu N (2009) Contamination of seismicity catalogs by quarry blasts: an example from Istanbul and its vicinity, Northwestern Turkey. *J Asian Earth Sci* 34:90–99. <https://doi.org/10.1016/j.jseaes.2008.03.012>
- Kekovalı K, Kalafat D, Kara M, Deniz P (2011) The estimation capability of potential mining and quarry areas from seismic catalog using statistical analysis, an application to Turkey. *Int J Phys Sci* 6(15):3704–3714
- Kim WY, Simpson DW, Richards PG (1994) High-frequency spectra of regional phases from earthquakes and chemical explosions. *Bull Seismol Soc Am* 84:1365–1386
- Kiszely M, Györi E (2015) Separation of quarry blasts from the aftershock sequence of the Oroszlány (Hungary) January 29, 2011 ML = 4.5. *Acta Geod Geophys* 50:97–107. <https://doi.org/10.1007/s40328-014-0078-0>
- Koch K, Fah D (2002) Identification of earthquakes and explosions using amplitude ratios: the Vogtland area revisited. *Pure Appl Geophys* 59:735–757
- Kortstöröm J, Uski M, Tiira T (2016) Automatic classification of seismic events with a seismograph network. *Comput Geosci* 87:22–30
- Nalbant SS, Hubert A, King GCP (1998) Stress coupling between earthquakes in northwest Turkey and the north Aegean Sea. *J Geophys Res* 103:24 469–24 486
- Ögütçü Z, Horasan G, Kalafat D (2011) Investigation of micro seismic activity sources in Konya and its vicinity, Central Turkey. *Nat Hazards* 58:497–509
- Pondard N, Armijo R, King GCP, Meyer B, Flerit F (2007) Fault interactions in the Sea of Marmara pull-apart (North Anatolian Fault): earthquake clustering and propagating earthquake sequences. *Geophys J Int* 171(3):1185–1197
- Reilinger R, McClusky S, Vernant P, Lawrence S, Ergintav S, Cakmak R, Ozener H, Kadirov F, Guliev I, Stepanyan R, Nadariya M, Hahubia G, Mahmoud S, Sakr K, ArRajehi A, Paradissis D, Al-Aydrus A, Prilepin M, Guseva T, Enren E, Dmitrotsa A, Filikov SV, Gomez F, Al-Ghazzi R, Karam G (2006) GPS constraints on continental deformation in the Africa-Arabia-Eurasia continental collision zone and implications for the Dynamics of plate interactions. *J Geophys Res* 111:B05411. <https://doi.org/10.1029/2005JB004051>
- SAC Seismic Analysis Code SAC 2000 Manuel, Lawrence Livermore National Laboratory, <http://www-ep.es.llnl.gov/www-ep/esd/seismic/sac.html>. Accessed 10 Oct 2017
- Şaroğlu F, Emre O, Kuşçu İ (1992) Active fault map of Turkey. Publ of General Directorate of Miner Res Explor Inst Turk Ankara
- SPSS V21 (2012) Statistical Package for the Social Sciences for Windows. IBM SPSS statistics
- Taylor SR, Denny DM, Vergino ES, Glaser RE (1989) Regional discrimination between NTS-explosions and earthquakes. *Bull Seismol Soc Am* 79:1142–1176
- Tibi R, Bock G, Xia Y, Baumbach M, Gresser H, Milkereit C, Karakisa S, Zünbül S, Kind R, Zschau J (2001) Rupture processes of the 1999 August 17 Izmit and November 12 Duzce (Turkey) earthquakes. *Geophys J Int* 144:F1–F7

- Wiemer S, Baer M (2000) Mapping and removing quarry blast events from seismicity catalogs, short notes. *Bull Seismol Soc Am* 90:525–530
- Wüster J (1993) Discrimination of chemical explosions and earthquakes in central Europe a case study. *Bull Seismol Soc Am* 83:184–1212
- Yalınrak C, İşler EB, Aksu AE, Hiscott RN (2012) Evolution of the Bababurnu Basin and shelf of the Biga Peninsula: western extension of the middle strand of the North Anatolian Fault Zone, Northeast Aegean Sea, Turkey. *J Asian Earth Sci* 57:103–119
- Yılmaz Ş, Bayrak Y, Çınar H (2013) Discrimination of earthquakes and quarry blasts in the eastern Black Sea region of Turkey. *J Seismol* 17:721–734. <https://doi.org/10.1007/s10950-012-9348-x>
- Zeiler C, Velasco AA (2009) Developing local to near-regional explosion and earthquake discriminants. *Bull Seismol Soc Am* 99:24–35